$K_4Au(TlSn_3)$: A Novel Zintl Phase with an Anionic Chain

Daping Huang and John D. Corbett*

Ames Laboratory-DOE[1] and Department of Chemistry, Iowa State University, Ames Iowa 50011

Received May 22, 1998

Reactions of the component elements at 1050 °C and then 400 °C in Ta containers generate the black title phase in good yield. Single-crystal X-ray characterization (monoclinic, *C*2/*c*, $Z = 4$, $a = 15.101(3)$ Å, $b = 6.6925(9)$ Å, $c = 14.389(3)$ Å, $\beta = 118.61(1)°$) revealed a novel infinite chain structure in which $\sim D_{2d}\ {}^{1}_{\infty}[(TlSn_3)Au]^{4-}$ units are made from tetrahedra of disordered Tl + 3Sn that are bridged at opposite edges by four-bonded Au atoms, and vice versa. The chains have the electron count of a classical Zintl phase in which all elements are four-bonded. The MOs of the chain fragment and the band structure of the chains are described. A relatively large gap appears to arise because of the similar energies of Au 6s and the $TlSn_3^{4-}$ units.

Introduction

Compounds formed between the alkali metals and the triel (Tr = Ga, In, Tl) elements have in the past few years proven to be a "gold mine" in the myriad of new and novel polyatomic cluster anions, both isolated and networked.[2] These include not only classic examples of the adherence to Wade's rules insofar as skeletal electron counts, in In_4^{8-}, Tl_5^{7-} and Tl_6^{8-}, for example, but also new distorted and hypoelectronic members as Tr_{11}^{7-} (D_{3h}), the self-centered icosahedral Tl_{13}^{11-}, and its fragment Tl_9^{9-}.[3] Centering of heteroatoms also affords stability with fewer electrons, as for $Tr_{10}Zn^{8-}$ and $Tr_{10}Ni$.[10−] While Wade's rules have been generally applicable in these instances in a structural sense, modest metal-like resistivities are sometimes encountered for what are still diamagnetic phases.[4] In addition, effective cation−anion packing in a few of these polar phases containing closed-shell anions may also afford structures that contain extra alkali-metal cations plus free electrons, as in $(A^+)_8(Tr_{11}^{7-})e^{-}$ [4,5] and $(K^+)_{18}Tl_{11}^{7-}(Tl_9Au_2^{9-})(Au^-)e^-$.[6] The last species illustrates the novelty that gold may bring to these systems. In $Tl_9Au_2^{9-}$, two gold atoms can be imagined to have substituted on the 3-fold axial positions of the pentacapped-trigonal-prismatic Tl_{11}^{7-}. A closed-shell configuration for the new cluster is then gained through both a strong axial compression that generates a transannuallar Au−Au bond ($d = 2.96$ Å) and the addition of two electrons.

The present article reports a different and novel result when both gold and the more electron rich tin are present, $K_4(AuTlSn_3)$. The repeat unit in the $AuTlSn_3^-$ chain is only one electron richer than the average Tl^- oxidation state already known in the homoatomic anion in $(K^+)_6Tl_4^{6-}$, a tetragonally compressed octahedron (square bipyramid).[7]

Experimental Section

Syntheses. The general techniques were as previously described.[4−7] All materials were handled in a N_2-filled glovebox with a moisture level below 0.1 ppm by volume. What by chance turned out to be the correct stoichiometric amounts of Au (reagent grade), Tl (99.998%), and Sn (99.999%, all from Johnson-Matthey) were first welded into a 9 mm diameter tantalum tube under Ar, and this was sealed under vacuum within a fused silica jacket. The assembly was heated at 1050 °C for 2 days and cooled in air. The resulting alloy pellet and the appropriate amount of K (99.9%, Baker) were then similarly enclosed in a second Ta/SiO_2 container, which was held at 400 °C for 4 days and then cooled to ambient temperature at 1 °C h^{-1}. Black barlike crystals of the title phase with obvious fibrous cleavage were obtained in 90% yield. Repeat reactions gave yields of ∼95% (in equivalent scattering power) according to the product's powder pattern.

The direct reaction of the elements at 400 °C is slower, requiring more than 25 days followed by slow cooling for a 90% yield. However, such a sample yielded an unknown phase when heated directly to 700 °C and then slowly cooled from 500 °C.

EDS. The elemental composition of a single crystal of the title phase was estimated with the aid of energy-dispersive X-ray spectroscopy (EDS) on a JEOL 840A SEM with a IXRF system X-ray analyzer and a Kevex Quantum light-element detector. A beam of 20 kV and 0.3 nA for a count rate of about 2500 s^{-1} was employed on the faces of a single crystal cleaved first in the glovebox. The EDS study yielded the approximated proportions of K:Au:Tl:Sn of 41:13:11:34 ≃ 3.6:1.1:1:3, with other elements undetected.

X-ray Diffraction. A selected crystal sealed in a thin-walled capillary within a glovebox was first checked by Laue photos for singularity and then mounted on a Rigaku AFC6R diffractometer for data collection with graphite-monochromated Mo Kα radiation. A least-squares refinement of the settings of 25 reflections from random searching in the range $14° < 2\theta < 20°$ provided a *C*-centered monoclinic cell with dimensions of about $a = 15.136$ Å, $b = 6.690$, $c = 14.37$ Å, and $\beta = 118.4°$. One hemisphere of data ($\pm h,k,\pm l$) was collected at room temperature out to $2\theta_{max} = 60°$ with an $\omega-2\theta$ scan mode, the *C*-centering condition being checked for the first 300 reflections. The intensities of 3 standard reflections checked every 150 reflections showed no significant decay or crystal motion.

The data were reduced and corrected for absorption with the aid of three ψ-scans.[8] Absences in the data set indicated that the *C*2/*c* space group was applicable. The first part of the structure solution came from direct methods[9] and yielded reasonable assignments for one gold

(1) This research was supported by the Office of the Basic Energy Sciences, Materials Sciences Division, U. S. Department of Energy. The Ames Laboratory is operated by DOE by Iowa State University under Contract No. W-7405-Eng-82.
(2) Corbett, J. D. In *Chemistry, Structure and Bonding of Zintl Phases and Ions*; Kauzlarich, S. M., Ed.; VCH: New York, 1996; Chapter 3.
(3) Corbett, J. D. *Struct. Bonding* **1997**, *87*, 157.
(4) Dong, Z.-C.; Corbett, J. D. *J. Cluster Sci.* **1995**, *6*, 187.
(5) Sevov, S. C.; Corbett, J. D. *Inorg. Chem.* **1991**, *30*, 4875.
(6) Dong, Z.-C.; Corbett, J. D. *Inorg. Chem.* **1995**, *34*, 5042.
(7) Dong, Z.-C.; Corbett, J. D. *J. Am. Chem. Soc.* **1993**, *115*, 11299.
(8) *TEXSAN*, version 6.0 package; Molecular Structure Corp.: The Woodlands, TX, 1990.

S0020-1669(98)00579-5 CCC: $15.00
Published on Web 09/04/1998

Table 1. Data Collection and Refinement Parameters for $K_4Au(Sn_3Tl)$

fw	913.81
cryst syst	monoclinic
space group, Z	$C2/c$ (No.15), 4
lattice constants[a]	
a (Å)	15.101(3)
b (Å)	6.6925(9)
c (Å)	14.389(3)
β (deg)	118.56(1)
V (Å^3)	1277.2(4)
temp (°C)	23
d_{calcd} (g/cm^3)	4.752
μ (Mo Kα) (cm^{-1})	310.45
$R1(F)$/wR2(F^2)[b] ($I > 2\sigma(I)$) (%)	3.83/8.44
$R1(F)$/wR2(F^2) ($I > 0$) (%)	6.79/9.40

[a] Guinier powder pattern data, $\lambda = 1.540\,562$ Å, 23 °C. [b] $R1 = \sum||F_o| - |F_c||/\sum|F_o|$; $wR2 = \{w[\sum(F_o^2 - F_c^2)^2]/\sum[w(F_o^2)^2]\}^{1/2}$, $w = 1/[\sigma^2(F_o^2) + (aP)^2 + bP]$, $P = [2F_c^2 + \mathrm{Max}(F_o^2,0)]^{1/3}$.

Table 2. Atomic Positions, Thermal Factors, and Occupancies for $K_4Au(TlSn_3)$

atom	x	y	z	U_{iso}[a]	occ
Au1	0	0.72829(8)	1/4	0.0266(2)	1
Sn1	0.41019(4)	−0.07831(9)	0.13350(4)	0.0232(2)	0.829(7)
Tl1	0.41019(4)	−0.07831(9)	0.13350(4)	0.0232(2)	0.171(7)
Sn2	0.58171(4)	0.62268(8)	0.20927(4)	0.0249(2)	0.674(7)
Tl2	0.58171(4)	0.62268(8)	0.20927(4)	0.0249(2)	0.326(7)
K1	0.6463(2)	0.1093(4)	0.1478(2)	0.0311(5)	1
K2	0.3514(2)	0.4309(4)	0.0035(2)	0.0337(5)	1

[a] $U_{iso} = 1/3\sum_i\sum_j U_{ij}a_i^*a_j^*a_ia_j$.

and two tin atoms. The structure was briefly refined using full-matrix least squares on F^2 for all data, after which two K atoms were assigned on the basis of the difference Fourier map. The composition at this point was K_4AuSn_4, without thallium. However, the ΔF map showed two fairly large residual peaks of about 8−9 e/Å^3 close to the assigned Sn1 and Sn2 sites and a −4.9 e/Å^3 hole near Au. These characteristics coupled with the EDS results indicated that the assigned Sn positions must actually have a mixed occupation by Tl atoms as well. The scale factor was evidently soaking up much of the error with only modest increases in B values of the other atoms. Refinement of the two sites with mixed Sn, Tl (=M) occupancies (the sum constrained to unity) gave a converged anisotropic refinement for the formula $K_4Au(Sn_{3.01(3)}Tl_{0.99(3)})$ with $R/R_w(F^2) = 6.79/9.37\%$ for all data ($I > 0$) and 3.83/8.44% for $I > 2\sigma_I$. The largest residual peaks, +2.51 and −2.78 e/Å^3, were 0.82 Å from M2 and 0.87 Å from Au, respectively. Refinement of the data set with $1/\sigma_{F^2}$ weights instead (Table 1) gave substantially the same numerical results and somewhat lower residuals, but the errors were slightly larger.

Some data collection and refinement parameters are listed in Table 1. The atomic positions, refined occupancies, and isotropic-equivalent displacement parameters are listed in Table 2, and the closer interatomic distances and some angles appear in Table 3. Additional information on the crystallography as well as the anisotropic displacement data are contained in the Supporting Information. The F_o/F_c listing and other information are also available from J.D.C.

Calculations. Extended Hückel MO and band calculations were carried out for the anion using the suite of programs developed by Hoffmann and co-workers at Cornell University. The orbital size parameters employed were their default values, while the H_{ii} parameters came from density functional theory (Sn s, −14.15 eV; Sn p, −7.31; Au 6s, −7.79; Au 6p, −4.14; Au 5d, −14.61).[10] The mixed Sn_3Tl positions were assigned as Sn atoms in the calculations, but the valence electron count employed was for the mixed atoms. The essence of the bonding was achieved with an idealized D_{2d} model in which the M_4 units were tetrahedral and all bond type distances were the averages of the observed values. Calculations were carried out both with and without the low-lying Au 5d orbitals. The energies of the bonding MO's for the $Au_{1/2}-M_4-Au_{1/2}$ repeat unit were taken as those at the Γ point in the band structure results.

Table 3. Interatomic Distances[a] (Å) and Selected Bond Angles (deg) in $K_4(AuTlSn_3)$[b]

Au1−M1	2.8219(8) (2×)	Au1−K1	3.366(2) (2×)
Au1−M2	2.8415(7) (2×)	Au1−K2	3.338(2) (2×)
M1−Au1	2.8219(8)	M1−K1	3.722(2)
M1−M2	2.9787(9)	M1−K2	3.609(2)
M1−M2	3.0335(9)	M1−K2	3.673(3)
M1−M1	3.147(1)	M1−K2	3.783(3)
M1−K1	3.692(2)		
M2−Au1	2.8415(7)	M2−K1	3.628(2)
M2−M1	2.9787(9)	M2−K1	3.789(2)
M2−M1	3.0335(9)	M2−K2	3.558(2)
M2−M2	3.198(1)	M2−K2	3.671(2)
M2−K1	3.610(2)		
K1−Au1	3.366(2)	K1−M1	3.722(2)
K1−M2	3.610(2)	K1−M1	3.692(2)
K1−M2	3.628(2)	K1−K2	3.779(3)
K1−M2	3.789(2)		
K2−Au1	3.338(2)	K2−M2	3.558(2)
K2−M1	3.609(2)	K2−M2	3.671(2)
K2−M1	3.673(3)	K2−K1	3.779(3)
K2−M1	3.783(3)		

M1−Au1−M1	67.78(3)	Au1−M1−M1	56.11(1)
M1−Au1−M2	134.14(2)	M2−M1−M1	59.29(2)
M1−Au1−M2	132.53(2)	M2−M1−M1	57.59(2)
M1−Au1−M2	132.53(2)	Au1−M2−M1	105.24(2)
M1−Au1−M2	134.14(2)	Au1−M2−M1	103.83(2)
M2−Au1−M2	68.50(3)	M1−M2−M1	63.11(3)
Au1−M1−M2	105.84(2)	Au1−M2−M2	55.75(1)
Au1−M1−M2	104.41(2)	M1−M2−M2	58.70(2)
M2−M1−M2	64.27(2)	M1−M2−M2	57.04(1)

[a] M = Tl + Sn (Table 2). [b] Distance cutoff 3.80 Å.

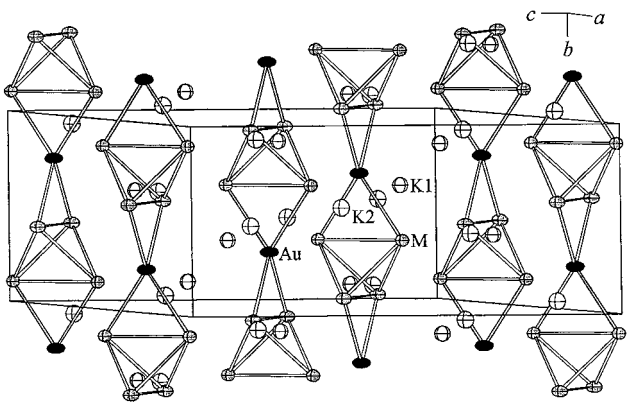

Figure 1. Portions of the $[Au(TlSn_3)]^{4-}$ chains around one cell in $K_4AuTlSn_3$ (90% probability ellipsoids). The gold atoms are black, and the disordered Tl and Sn atoms are shaded.

Results and Discussion

Structure. The compound $K_4AuTlSn_3$ exhibits a unique structure in which the heavy elements form infinite one-dimensional chains $^1_\infty[Au(TlSn_3)]^{4-}$. Figure 1 shows portions of several chains relative to the unit cell, while Figure 2 shows the independent distances in the repeat unit. The chains are built of approximate M_4 tetrahedra of disordered Tl + 3Sn atoms (M) that are interbridged on opposed edges by μ_4-gold atoms. Gold likewise centers a very elongated M_4 tetrahedron, and the chain construction could also be described as

(9) Sheldrick, G. M. *SHELX-97*; Universität Göttingen, Göttingen, Germany, 1997.
(10) Vela, A.; Gazquez, J. L. *J. Phys. Chem.* **1988**, *92*, 5688.

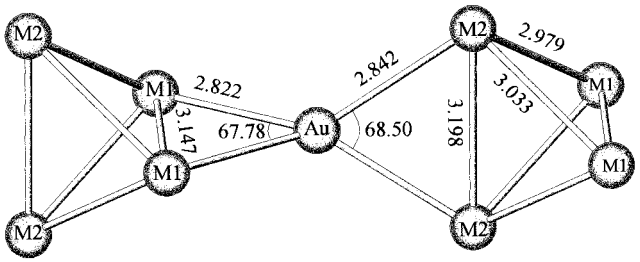

Figure 2. Segment of one chain in $K_4Au(TlSn_3)$ with the independent distances marked.

$^1_\infty[(M1)_2Au(M2)_2]^{4-}$ units in which pairs of M1 and M2 with alternating ~90° orientations along an S_4 axis generate M_4 tetrahedra. Pairs of chains in the *C*-centered monoclinic cell ($\beta = 118.6°$) can be seen in Figure 1 to lie at 0, *y*, 1/4 and 1/2, $\bar{y}$, 3/4 with the gold atoms at $y \sim 3/4$, while the second pair of chains is related by inversion through 0, 0, 0 or the equivalent. The result is roughly a 2-D arrangement of close-packed chains along $\bar{b}$ in a pseudohexagonal cell. As will be shown, the compound is closed-shell and therefore a Zintl phase.

The M_i-M_i dimers just described show distances of 3.147(1) Å (M1−M1) and 3.198 (1) Å (M2−M2), while the distances between these along the chain are 2.979(1) and 3.034-(1) Å. In other words, the $TlSn_3$ tetrahedra are slightly compressed along the chains. These distances are appropriately a little bit longer than *d*(Sn−Sn) about four-bonded (4b) tin in K_8Sn_{44} (2.84 Å)[11] and in the more strained Na_5Sn_{13} (2.92 Å).[12] The refined amount of Tl on the M2 sites, 33%, is distinctly greater than at M1, 17%, and the Au−M distances are in parallel, that to M2 being 0.020 Å longer, but this is still 0.03 Å shorter than *d*(Tl−Au) in the anion $Tl_9Au_2^{9-}$.[6] The asymmetric distribution of Tl on M1 and M2 is presumably correlated with, or caused by, the cation distribution. The five or six K ions about each M lie distinctly closer to the Tl-poorer M1, by an average of 0.07 Å, the smaller size of tin evidently being more influential than the formal −1 charge borne by thallium. Elongation of the tetrahedron about gold is a consequence of the combination of intrinsic *d*(Au−Sn(Tl)) lengths (~2.83 Å) with the *d*(M_i-M_i) value for the bridged edges of the M_4 unit, 3.15−3.20 Å. The ellipsoids of the M atoms are slightly elongated in a tangential way that would suggest either small torsional displacements around the chain axis or, probably more likely, the statistical result of small differences in Sn−Sn, Sn−Tl, and Tl−Tl bond lengths.

It should be noted that the refined composition of the atoms in the tetrahedra, $Tl_{0.99(3)}Sn_{3.01(3)}$, corresponds to the ideal formula $K_4Au(TlSn_3)$ within experimental error. This is furthermore just the composition for a classical Zintl phase with two-center−two-electron bonding following the octet rule. This is seen most easily in the von Schnering notation,[14] in which electron transfer from the electropositive potassium to the chain generates (in terms of oxidation numbers) the closed-shell representation (4b-Au^{-3})(4b-Tl^-)(4b-Sn^0)$_3$, i.e., $[Au(TlSn_3)]^{4-}$ in which all atoms are bonded to four neighbors in roughly tetrahedral configurations.

Isoelectric examples of the same chain motif in the series $A_3(AuTt_4)$ (A = K, Rb, Cs; Tt = Sn, Pb) have recently been characterized by Zachwieja and co-workers.[15] The largest difference on exchange of tin for the one atom of thallium is a change of the packing to that of the orthorhombic *Pmmn* ($Z = 4$) with three rather than four cations per chain unit. Both types of chain compounds may be related (somewhat distantly) to the structure of $SiS_{4/2}$, where SiS_4 tetrahedra share trans edges. Removal of every other Si and condensation of the fragments into tetrahedra would give the present result. A relationship also exists with the dimeric Ge_8Zn^{6-} units found in the Zintl phase Cs_6Ge_8Zn.[16] These are derived from pairs of classic Ge_4^{4-} tetrahedra that are interbridged through faces by Zn^{2+}. The six-bonded zinc is logically replaced by four-bonded, edge-bridging gold here.

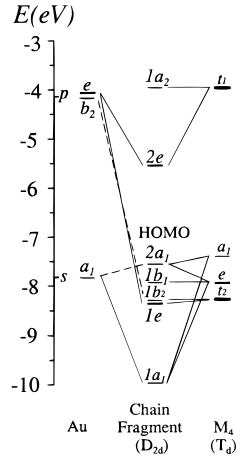

Figure 3. The extended Hückel molecular orbital diagram for the anion chain fragment in $K_4Au(TlSn_3)$, idealized to D_{2d} symmetry, without the small effects from Au 5d around −14.6 eV. Tin orbital parameters were used for all atoms in the tetrahedron.

Bonding. An approximate local bonding picture for an idealized [$Au_{1/2}-M_4-Au_{1/2}$] unit in the chain with D_{2d} symmetry with all M = Sn is shown in Figure 3. The low-lying Sn 5s orbitals (−14.2 eV) and gold 5d (−14.61 eV) are not plotted, and their principal interactions are with each other. The $1b_2$, $1b_1$, and HOMO $2a_1$ MO's in the chain fragment are important for bonding within M_4 but are substantially nonbonding to Au, though a small amount of Au d_{xy} contributes to $1b_2$. On the other hand, the MOs $1a_1$ and 1e are largely responsible for the bonding between Au and M_4. According to the bonding contributions in this region at Γ shown in **I**, $1a_1$ features Au

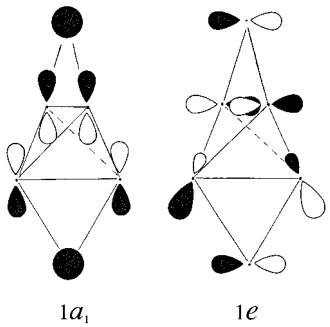

I

s−M p_z σ bonding and M−M σ ($+\pi$) bonding, while 1e contains σ bonding between Au p, d_{xy}, and M p_z on one side but π^* interactions on the other side. The d_{xz} and p_x orbitals on Au contribute about equally in 1e (not shown). This d mixing affords the only visible change in the band structure of

(11) Zhao, J.-T.; Corbett, J. D. *Inorg. Chem.* **1994**, *33*, 5721.
(12) Vaughey, J. T.; Corbett, J. D. *Inorg. Chem.* **1997**, *36*, 4316.
(13) Dong, Z. C.; Corbett, J. D. *Inorg. Chem.* **1995**, *34*, 5709.
(14) von Schnering, H.-G. *Angew. Chem., Int. Ed. Engl.* **1981**, *20*, 33.
(15) Zachwieja, U.; Müller, J.; Wlodarski, J. *Z. Anorg. Allg. Chem.* **1998**, *624*, 853.
(16) Queneau, V.; Sevov, S. C. *J. Am. Chem. Soc.* **1997**, *119*, 8109.

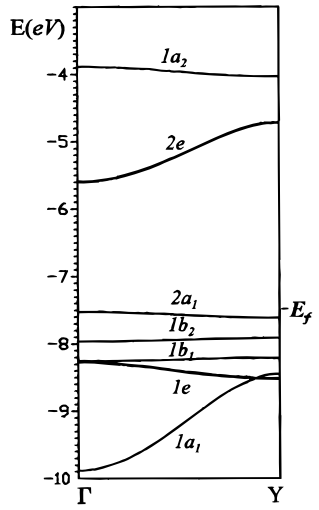

Figure 4. Band diagram for $^{1}_{\infty}[Au(TlSn_3)]^{4-}$.

the solid in the region of Figure 4, raising 1e at Γ by about 0.25 eV. The large dispersion for $1a_1$ and a small one for 1e in the band structure are opposed in bonding effects; that for $1a_1$ becomes less bonding at Y largely only within the shared edges when it contacts other "out of cell" tetrahedra, while 1e becomes somewhat more bonding within the tetrahedron (not shown).

The size of the gap (in the extended Hückel approximation) appears quite large for this sort of compound, and this originates mainly with the distribution of Au orbitals. Basically, the mid-lying Au 6s interacts well with only a_1 and e states derived from the M_4 tetrahedron and produces only one low-lying result, a_1. The remainder of the orbitals remain near the Au 6s energy and contain internal bonding in M_4 except for some a and e types for the M_4 tetrahedron that are pushed to much higher lying levels (off scale). Gold 6p (e) interacts principally with the antibonding t_1 level of M_4 to give the high-lying LUMO. These unusual circumstances thus appear responsible for the relatively large gap calculated, ∼1.9 eV. As might be expected, the barrier to a chain twist around gold is quite large.

These conclusions are of course conditioned by both the limits of the EHMO method and the reliability of the parameters, particularly for gold. The Au 6s orbital energy employed, −7.79 eV, is close to the relativistic value, −7.94 eV, but is still some distance from the experimental value of $-I_1$, 9.92 eV.[17] However, their choice is made moot by expected increases in the valence state energies for all atoms in these polyanions, probably more so for gold.

A noteworthy contrast exists between these (and other) calculational results and the easy correlations made on the basis of structure and closed-shell octet (Zintl−Klemm) concepts that nonetheless seem to work so well. Thus, the present structure "makes sense" when it is simply described as 4b-Au^{3-}(4b-Tl^{-})-(4b-Sn^{0})$_3$ in terms of oxidation states, which gives suitable valence configurations for all atoms, ready for four covalent bonds. Of course, the implied charge transfer is too extreme, but the notion is still imparted that gold would utilize s and three p orbitals. The actual atom populations secured in a simple EHMO treatment (subject to the Mulliken approximation of dividing bond electrons equally) in fact give gold orbital populations of 5d, 9.92, but only 0.70 for s, 0.27 for p_z, and 0.16 each for the other p, for a total charge of $Au^{-0.21}$. The three Sn and one Tl in the tetrahedron have average charges of about −0.94 in the same approximations.

Acknowledgment. We are indebted to W. E. Straszheim for the EDS measurements and to Dr. U. Zachwieja for a copy of the manuscript for ref 15 prior to publication.

Supporting Information Available: Two tables of detailed data collection and refinement information and of the anisotropic displacement parameters for $K_4Au(TlSn_3)$ (2 pages). Ordering information is given on any current masthead page.

IC980579Q

(17) Pitzer, K. S. *Acc. Chem. Res.* **1979**, *12*, 271.